Reac Kinet Mech Cat (2015) 116:273–283
DOI 10.1007/s11144-015-0890-8

Effect of relative humidity on HCl formation from the reaction of H_2SO_4 and HNO_3 with NaCl particles

B. N. Fong[1] · K. V. Newhouse[2] · H. Ali[1]

Received: 25 February 2015 / Accepted: 24 May 2015 / Published online: 3 June 2015

Abstract Short path gas cell Fourier transform infrared spectroscopy was used to analyze the production of hydrochloric acid (HCl) gas from the reaction of sodium chloride (NaCl) particles and sulfuric acid (H_2SO_4) or nitric acid (HNO_3) at a range of relative humidity (2–95 %). HCl was produced from both acids, and reached equilibrium in 10 min for both H_2SO_4 and HNO_3 acids. The equilibrium is thought to be a result of two competing reactions which produce HCl and sequester it back into the NaCl particles. The HCl production from H_2SO_4 was instantaneous, but its production from HNO_3 involved an induction period of a few minutes. The equilibrium HCl conditions observed here have implications in influencing the pH of aerosol particles, and consequently the acidity of precipitation in the atmosphere.

Keywords Short path gas cell FT-IR · Sodium chloride · Relative humidity · Hydrochloric acid

Introduction

Hydrochloric acid (HCl) is an atmospheric acid playing a vital role in the overall budget of chlorine species in the atmosphere. A main source of gas phase hydrogen chloride (HCl) in the atmosphere is the reaction of sulfuric acid (H_2SO_4) and nitric acid (HNO_3) with metallic chlorides, most commonly NaCl, primarily produced from sea salt aerosols [1]. This degassing from sea-salt produces about (50 ± 20) teragram (1×10^9 kg = 1 Tg) of HCl per year. Another large source

✉ H. Ali
hali@astate.edu

[1] Department of Chemistry and Physics, Arkansas State University, State University, AR 72467, USA

[2] Department of Math and Science, University of Arkansas at Monticello, Monticello, AR 71656, USA

of HCl is coal combustion sources (4.6 ± 4.3) Tg year^{-1} [2], acid displacement reactions (7.6 Tg year^{-1}) [3] and chlorocarbons from the stratosphere (4.2 Tg year^{-1}), [4]. The sources of H_2SO_4 and HNO_3 acids are usually from the reaction of SO_x and NO_x species with water vapor in the atmosphere.

The reaction of H_2SO_4 and HNO_3 with NaCl has been studied before. These studies focused mainly on the uptake and reaction of these acids with the salt and found HCl as a gas byproduct of all these reactions. The production of HCl is important to study because it is the main source of chlorine in the atmosphere which eventually determines the tropospheric ozone concentrations [5]. Gas phase HCl can also be wet-deposited back into the ground by accumulating in soil and lakes, affecting the pH and damaging processes that are vital for plant and animal health [6].

The production of HCl from the reaction of H_2SO_4, HNO_3 with NaCl is proposed to occur in the following pathways [7]:

$$2NaCl_{(s)} + H_2SO_{4(aq)} \rightarrow Na_2SO_{4(s)} + 2HCl_{(g)} \quad (1)$$

$$NaCl_{(s)} + HNO_{3(aq)} \rightarrow NaNO_{3(s)} + HCI_{(g)} \quad (2)$$

The kinetics of the formation of HCl from Eq. 1 has been studied at 600 °C and in the absence of water vapor [8]. They found that the rate of HCl production depended on the adsorption of SO_2 and H_2O and the formation of H_2SO_4 on the surface of NaCl particles. The role of water (as relative humidity, RH) in the production of HCl from these reactions is important to study because water vapor is ubiquitous in the atmosphere. The effect of humidity on HCl production has not been investigated before, to the best of the investigator's knowledge. Most of the reactions in the atmosphere are RH dependent, and this would mean that the production of HCl has to be RH dependent. For example, water vapor content (as RH) was found to increase the kinetics of the reaction between NaCl and nitrogen oxide species using a Knudsen Cell reactor [9]. Ali et al. 2014, determined NaCl particles at 84 % RH exposed to sulfuric acid completely convert to Na_2SO_4 after 30 min with the release of HCl [10]. All these experiments focus on the chemical characteristic changes of NaCl particles as a function of RH, but not on the influence of RH on the production of HCl gas, the other product from these reactions.

In this study, the production of HCl(g) from the reactions of H_2SO_4 and HNO_3 with sodium chloride particles is investigated as a function of humidity using short path gas cell Fourier transform infrared (FTIR) spectroscopy. Changes to the NaCl particles were not monitored as these studies have been done in detail by previous researchers.

Materials and methods

Sodium chloride (reagent grade) was purchased from Carolina Biological Supply Company, Burlington, NC. Sulfuric acid (reagent ACS grade) and nitric acid (certified ACS grade) were purchased from Fischer Scientific, Fairlawn, NJ.

Sodium chloride particles were placed in a reaction chamber (250 mL) and exposed to either sulfuric acid (H_2SO_4) or nitric acid (HNO_3) at varying relative humidity (Fig. 1). The RH from the experiments was controlled by mixing dry and wet air from two bubblers placed before the experimental setup. Dry air came from a commercial air dryer (Kaeser, KADW series).Wet air was created by bubbling dry air through two Pyrex 500 mL gas washing bottles with coarse fritted discs and 40/50 glass stoppers (Corning, 31760-500C).The relative humidity was measured with an RH sensor (Sensiron, EKH4) mounted in the air flow line before the reaction chamber to minimize damage to the sensor. A syringe tip with a septum allowed for a syringe to directly inject the acid into the reaction chamber. Gas phase species produced were analyzed using a commercial 100 mm short path gas cell (Pike Technologies, 162-2200) placed into the internal compartment of the spectrometer by a slide mount accessory. The gas cell was fitted with two Viton O-rings (Pike Technologies, 162-2209) and 38 × 6 mm Zn Sewindows (Pike Technologies, 160-1329) on each side so that the IR beam passes through two windows. Infrared spectra were collected using a single beam Thermo Scientific Nicolet 8700 FT-IR spectrometer with liquid nitrogen-cooled mercury–cadmium–telluride (MCT) detector and KBr beam splitter. Typically 100 scans were averaged at a 4 cm^{-1} instrument resolution over the 400–4000 cm^{-1} spectral range over 60 s. The gas cell was connected to a flow system and reaction chamber via Swagelok PFA tubing (OD 250″) and adapters (Fig. 1). A commercial air dryer (Kaeser, KADW series) removed carbon dioxide and water vapor, purged the FT-IR system and provided dry (<1 % RH) air for the flow system.

Before each experiment, dry air (<1 % RH) was purged into the system for 5 min to clean the system and remove any moisture in the lines. Then, 2 g of sodium chloride particles was added to the reaction chamber. For all experiments, the RH was adjusted to within 1 % and allowed to equilibrate for 2 min. Air flow was shut off, valves closed and 2–3 mL of acid was added to the reaction chamber to start the reaction. The rate of gas production was measured by taking IR scans every other minute for 30 min. The scans take 1 min to complete, and a 1 min delay was taken between each sample.

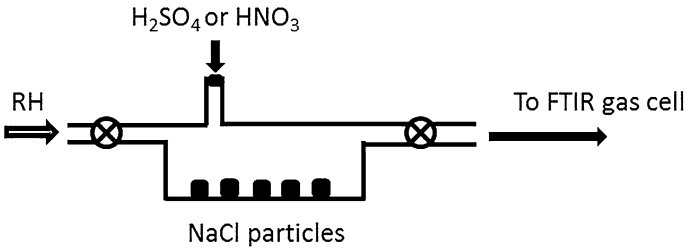

Fig. 1 Schematic of the reaction chamber used to investigate the production of gas phase HCl at a range of relative humidity. The gas cell and IR spectrometer follow immediately after the reaction chamber and are not shown here

Results and discussion

H_2SO_4 with NaCl as a function of RH

The sulfur (IV) uptake as SO_2 and conversion to S(VI) creates a large sulfate fraction in clouds [11] that can react with water vapor to form sulfuric acid. These reactions lead to the formation of these strong acids and their subsequent reaction with aerosol particles like NaCl leads to the formation of salts like sodium sulfate and sodium bisulfate [10], with the accompanying production of gas phase HCl. When sulfuric acid was flown into our reaction chamber, gas phase HCl was observed in the IR spectrum as expected. The reaction is instantaneous because HCl gas is immediately observed when H_2SO_4 was introduced into the reaction chamber.

The IR spectrum of HCl(g) is well known and consists of two distinct regions, from 2500 to 2860 cm^{-1} and from 2900 to 3100 cm^{-1}. A representative spectrum at 30 % RH after 10 min is shown in Fig. 2. The peaks at 2940 and 2800 cm^{-1} are the two regions with the highest peaks measured in the gas phase, which match ab initio calculations from Herzberg [12]. The doublet characteristics of HCl absorptions are due to the natural isotopic abundance from ^{35}Cl and ^{37}Cl identified as P (at higher wavelength) and Q (at lower wavelength) branches of gas phase HCl species. The peaks are not equidistant because the separation decreases with increasing J (splitting distance) in the rigid rotator model. A line or peak is missing in the middle

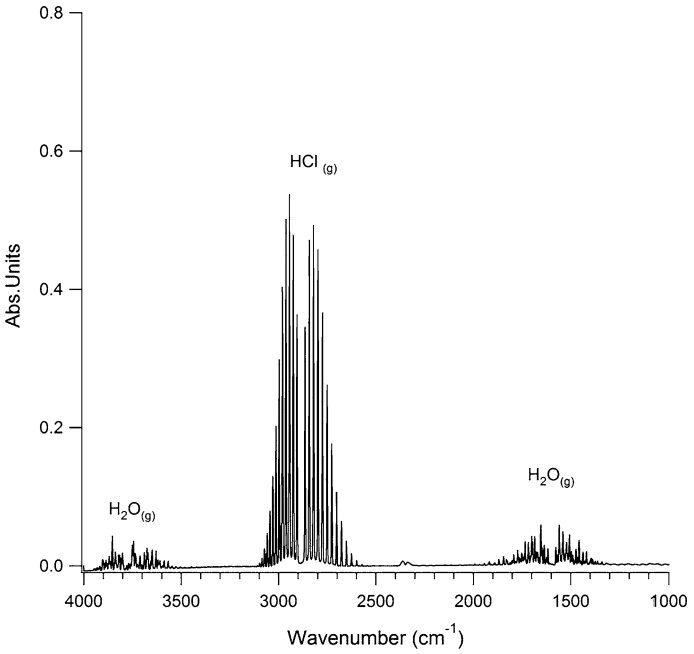

Fig. 2 Gas phase Infra-Red spectra of HCl at 30 % RH after 10 min. Peaks associated with gas phase HCl and H_2O are labeled, and are assigned in the text

due to the zero gap, where the molecule does not rotate.The other two smaller peaks are due to the *ro-vibrational* spectra of gas phase H_2O (RH here was at 30 % RH) from 1325 to 2020 cm^{-1} and from 3490 to 3940 cm^{-1}.The peak centered at 3780 cm^{-1} is the OH stretch and the peak centered around 1600 cm^{-1} is the OH bend in water vapor, indicating presence of gas phase water vapor in the chamber. These peaks match the assignments of water vapor in the gas phase [13].

The concentration of HCl produced from this reaction was monitored by acquiring the integrated absorbance from 3100 to 2500 cm^{-1} every 2 min throughout the reaction at different RH conditions (2–95 % RH) until equilibrium is achieved (at the plateau region).The integrated absorbance values were then converted to gas phase HCl concentration (as pressure P_{HCl}) by using a calibration curve and the Henrys Law constant of HCl (in aqueous phase) value of 19 M atm^{-1} [14]. Using the calibration data, the integrated absorbances for HCl were converted to P_{HCl} and values plotted. The HCl produced from different RH (2, 30, 50, and 85 %) are shown in Fig. 3. After 10 min, the reaction reaches a maximum equilibrium value (P_{eq}) of 0.46 ± 0.08 atm.

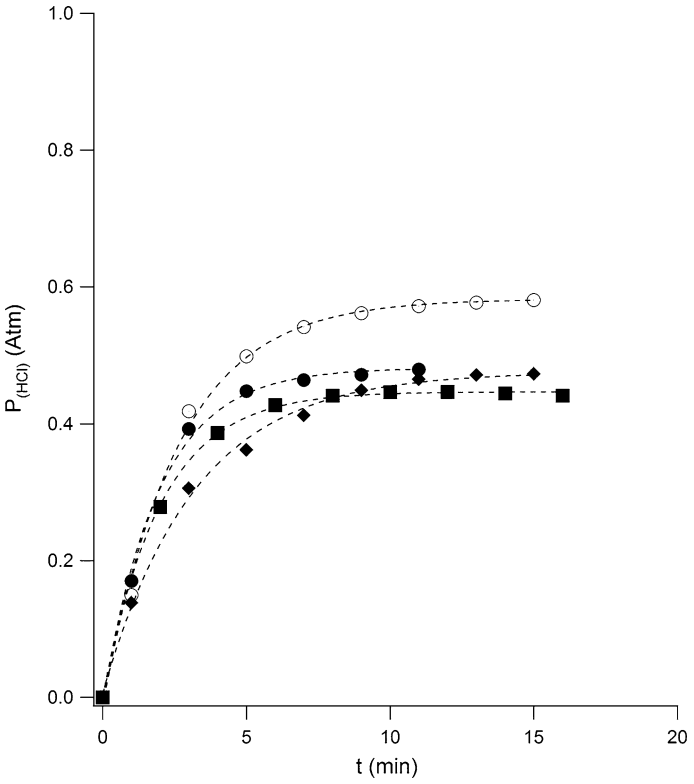

Fig. 3 Time lapse graph of the amount of HCl formed as a function of RH measured by integrated absorbance from 3100 to 2500 cm^{-1}. The relative humidity shown here are from 2 %RH (*dark diamonds*), 30 % RH (*dark squares*), 50 % RH (*dark circles*) and 85 % RH (*open circles*). Other RH values are not plotted for clarity

The curves were fitted to an exponential function following the formula below, to determine the P_{eq}:

$$P_{HCl} = P_{eq} + Ce^{\left[\frac{t_0 - t}{\tau}\right]} \quad (3)$$

where P_{eq} is pressure of HCl at equilibrium, t_0 is initial time (zero for our case) and *tau* (τ) is the HCl growth rate as function of time (atm min^{-1}).The curve fit equation produced R^2 value of >0.999 and were therefore utilized to investigate the P_{eq} of HCl as a function of RH. The HCl growth rates, measured as τ, from selected RH (2, 30, 50, and 85 %) are summarized in Table 1. When the P_{eq} value from all the RH investigated were plotted as function of RH, they all lined up within an average value of P_{eq} as seen in Fig. 4. As evident from the graph, the P_{eq} values were constant throughout the RH investigated, all reaching a similar P_{eq} with an average value of 0.46 ± 0.08 atm. The growth rates, although varying slightly, also show a similar average value (2.43 ± 0.58 atm min^{-1}), indicating a constant growth rate in HCl production with maximum HCl production reaching equilibrium at around 10 min (Fig. 3). This maximum HCl production condition has been seen before in the field. Pio and Harrision found that the concentration of gaseous compounds in the western coast of Iberian Peninsula steadily increased depending on air mass movement, with the exception of HCl, which increased steadily before reaching a constant maximum value [15]. The average P_{eq} values seen here indicate a presence of an equilibrium condition between two processes, one that produces HCl and one that removes/sequesters the HCl.

Zangmeister and Pemberton observed these processes occurring in the presence of water. In the presence of water vapor (as RH here), the reaction of sulfuric acid and NaCl may be enhanced, leading to an increase in the amount of HCl produced, seen here as the linear part of the exponential growth [16]. They also proposed that, since this reaction occurs in the particles, the HCl produced can also be sequestered inside the particle, reducing the amount produced by almost 40 %. Based on the kinetic data observed here, we believe that these two processes (enhancement and sequester) are competing reactions occurring throughout the RH investigated, leading to an equilibrium condition (equal rates of these two processes) achieved after 10 min. The consequence of these competing reactions is that the overall amount of HCl produced becomes independent of the amount of water vapor (as RH), and stays constant (at least in the duration of the experiments investigated here) as RH is changed. The reaction is expected to stop once all the chlorine in NaCl has been depleted. Since HCl is one of the main species contributing to the acidity of atmospheric particles, this constant equilibrium HCl production will lead

Table 1 The rate of growth of HCl (τ) as a function of time from the reaction of H_2SO_4 and NaCl

%RH	τ (atm min^{-1})
2	1.95 ± 0.16
30	2.01 ± 0.04
50	3.19 ± 0.19
85	2.58 ± 0.18

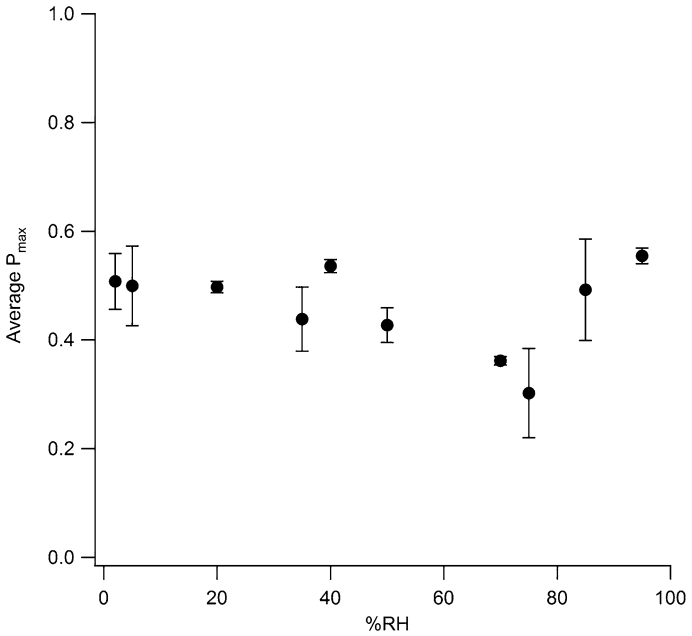

Fig. 4 Equilibrium pressures (P_{eq}) achieved after 10 min of the reaction between H_2SO_4 and NaCl plotted as function of relative humidity. The *black circles* are averages of at least triplicate measurements and their standard deviations

to a constant pH contributing effect, and will play a minor, if not smaller, role in the acidity of particles in the atmosphere and consequently to the acidity of rain.

HNO_3 with NaCl as a function of RH

The other important acid responsible for chloride depletion from sea salt and the production of HCl in the atmosphere is nitric acid (HNO_3). HNO_3 is formed from the reaction of nitrogen dioxide with OH in the atmosphere and is wet deposited back to earth in the form of acid rain. When nitric acid is added to sodium chloride particles, they produce gas phase HCl [9] and sodium nitrate as seen in Eq. 2 above. The HNO_3 also decomposes in the presence of water to release nitrogen oxide (NO) gas that was also observed in the spectrum (Fig. 5). NO was observed at 1802 cm^{-1}, supported by a yellow-brown gas product and vibrational calculations [17]. At higher RH, the NO gas was observed to react with the gas cell (ZnSe) windows. The windows turned brown, and the spectra show interference noted by a sloping baseline in the IR spectra (Fig. 5). The rounded peaks at 3375 and 1615 cm^{-1} indicate that liquid water, as condensation, deposit on the gas cell windows. The reaction of HNO_3 and NaCl particles was not investigated at higher RH to preserve the gas cell for future experiments.

When NaCl particles were exposed to a constant flow of HNO_3, there was a distinct lag or delay before the HCl gas phase spectra could be observed in the gas

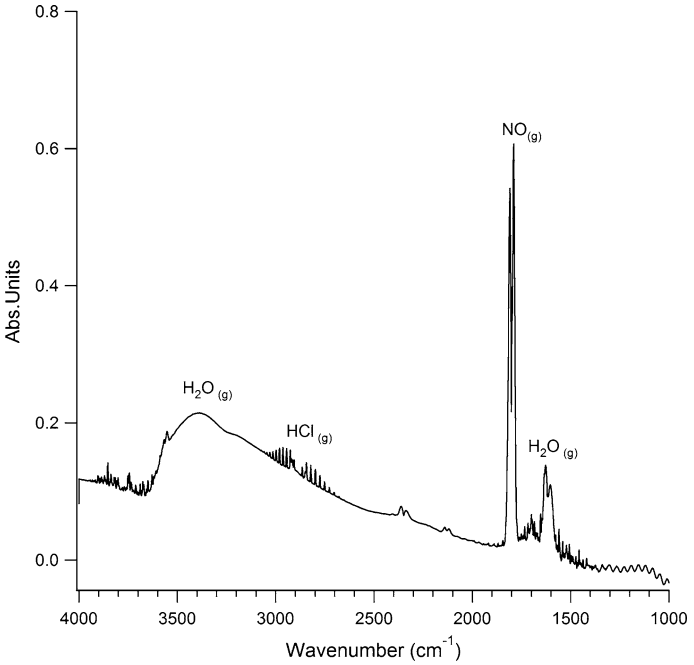

Fig. 5 Gas phase IR spectra of HCl produced from HNO_3 and NaCl at 30 % RH after 10 min. Peaks associated with gas phase HCl, H_2O and NO are labeled and assignments are in the text

cell and analyzed. This is seen in Fig. 6 for the HCl production from HNO_3. This lag was repeatedly observed on multiple experiments, and occurs in the first 5 min before HCl could be observed and analyzed. After 5 min of delay, the HCl gas phase spectrum was observed and grew steadily up to 15 min when the equilibrium was reached, an almost double the amount of time it took for the HCl from H_2SO_4 to reach equilibrium. The growth rate at this (30 %) RH taken from the data fit was calculated to be 4.25 ± 1.06 atm min^{-1}, almost double compared to the growth rate of HCl from H_2SO_4 reaction. As mentioned above, higher RH conditions could not be attempted because of the reaction of NO with gas cell windows interfering with the experiment.

A similar delay process observed here has been reported before, for the reaction of HNO_3 on NaCl in the presence of water vapor. In the presence of water vapor, water structures on the surface of NaCl crystals have been observed by several researchers [18–20]. They report that in early relative humidity conditions, these water structures create 2 dimensional (2D) structures and when the amount of water vapor is increased, change to 3 dimensional (3D) layers on the surface. This process takes a few seconds to a few minutes at the beginning of the reaction. We believe that the reaction of HNO_3 with NaCl does not occur until these 3D water layers have been formed, creating condensed phase necessary for the reaction to proceed. As these structures are being formed, they slow down the ionic mobility or dissolution of HNO_3 into the NaCl particles, slowing down HCl production as contact between

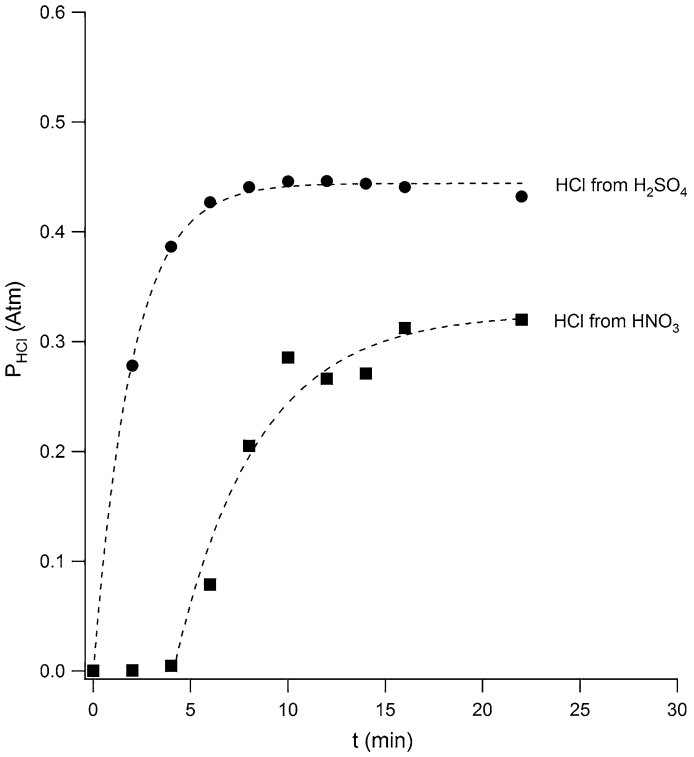

Fig. 6 Amount of HCl produced from reaction of NaCl with H_2SO_4 (*dark circles*) and HNO_3 (*dark squares*). The HCl production is higher from H_2SO_4, and is instantaneous. The HCl production from HNO_3 involves a delay observed in the first 5 min. See text for more details

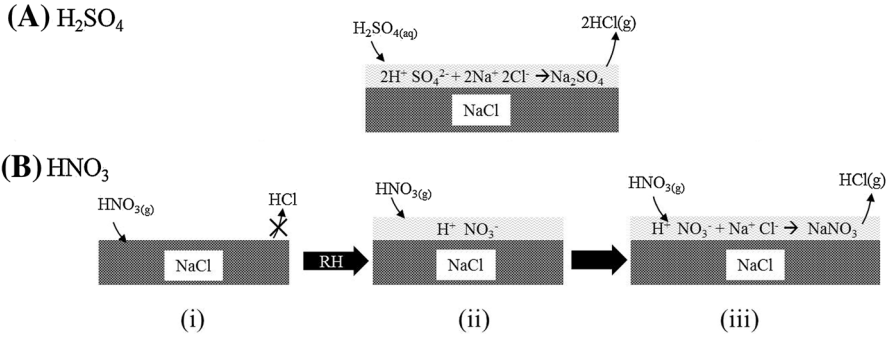

Fig. 7 Schematic diagram of the reaction mechanism of sulfuric (**a**) and nitric acid (**b**) onto sodium chloride particles. HCl is formed immediately after contact with H_2SO_4 because the acid is in the condensed phase. While initially the reaction of HNO_3 and NaCl does not occur in the induction phase (I). Between 2 and 30 %, water vapor is added to the sodium chloride particles in a layer addition phase (II). Once the layer of water develops the reaction of HNO_3 and NaCl can progress (III)

HNO_3 and NaCl is delayed, producing the 5-min delay in HCl production that is seen in Fig. 6.

Contrary to this, the hygroscopicity of H_2SO_4 acid means that this acid is always in the condensed phase. Since the reaction of H_2SO_4 with NaCl is already in a condensed phase, the reaction occurs immediately after the H_2SO_4 meets with NaCl, resulting in the absence of the delay as seen in Figs. 3 and 6. The importance of a condensed phase (of a water liquid layer) has been observed [21], where they found the reaction of sodium sulfate with HCl does not occur without the presence of water vapor. A model has been proposed for the reaction of HNO_3 with NaCl powders and involves rapid uptake of HNO_3 from the gas phase into the surface adsorbed water, leading to the increase in acidity of the surface and the release of HCl gas (Fig. 7b). This model suggests an induction period for the production of HCl, i.e. it will degas only until when the surface adsorbed water has become sufficiently acidic [22]. This first step may lead to the delay observed in our experiment.

P_{eq} from the fit of data for the reaction of HNO_3 with NaCl was found to be 0.33 ± 0.03 atm, slightly lower than that for the HCl production from H_2SO_4. The lower production rate is explained by the slower kinetics of HNO_3 with NaCl in comparison to H_2SO_4 with NaCl [23]. The slower rate leads to a lower P_{eq} for the HCl production as seen in Fig. 6 and a lower maximum HCl amount compared to the HCl from H_2SO_4 process. This implies that the role of H_2SO_4 in controlling the acidity of aerosol particles in the atmosphere is greater than that of HNO_3, with the contribution coming from its own acidity and its role in the production of higher HCl concentrations than those from HNO_3.

Conclusions

The production of HCl from the reaction of H_2SO_4 and HNO_3 under varying RH was investigated by short path length gas phase FT-IR spectroscopy. HCl produced from H_2SO_4 reactions was found to be independent of RH conditions. This independence is thought to be due to two competing processes: one enhances the production of HCl and another sequesters the produced HCl from the reaction, resulting in an equilibrium process observed after 10 min. The HCl production from HNO_3 was found to involve an induction period, where HNO_3 dissolution into 3D surface water structures slow down the contact with NaCl, long enough to create a delay, after which HCl gas is produced and reaches an equilibrium value that was lower than that from H_2SO_4 process. The atmospheric implications of this HCl equilibrium is that the pH of atmospheric particles do not depend on the contribution from HCl, and are solely dependent on the acidity of H_2SO_4 and HNO_3 and to a lower extent from HCl.

Acknowledgments Funding was provided by Arkansas Science Technology Authority (ASTA) summer internship program and Arkansas State University (ASU) faculty research awards. We would also like to acknowledge Dr. Ben Rougeau for his continued support with instrument calibrations.

References

1. Graedel TE, Keene WC (1995) Tropospheric budget of reactive chlorine. Glob Biogeochem Cycles 9:47–77. doi:10.1029/94GB03103
2. McCulloch A, Aucott ML, Benkovitz CM et al (1999) Global emissions of hydrogen chloride and chloromethane from coal combustion, incineration, and industrial activities: reactive Chlorine Emissions Inventory. J Geophys Res 104:8391–8403
3. Erickson DJ, Seuzaret C, Keene WC, Gong SL (1999) A general circulation model based calculation of HCl and $ClNO_2$ production from sea salt dechlorination: reactive Chlorine Emissions Inventory. J Geophys Res 104:8347. doi:10.1029/98JD01384
4. Sanhueza E (2001) Hydrochloric acid from chlorocarbons: a significant global source of background rain acidity. Tellus B 53:122–132. doi:10.1034/j.1600-0889.2001.d01-11.x
5. Finlayson-Pitts BJ, Pitts JNJ (2000) Chemistry of the upper and lower atmosphere: theory, experiments, and applications, 1st edn. Academic Press, San Diego
6. Eldering A, Solomon PA, Salmon LG et al (1991) Hydrochloric acid: a regional perspective on concentrations and formation in the atmosphere of Southern California. Atmos Environ Part A 25:2091–2102. doi:10.1016/0960-1686(91)90086-M
7. Tang IN, Tridico AC, Fung KH (1997) Thermodynamic and optical properties of sea salt aerosols. J Geophys Res 102:23269–23275. doi:10.1029/97JD01806
8. Henriksson M, Warnqvist B (1979) Kinetics of the formation of HCl(g) by the reaction between NaCl(s) and SO_2, O_2, and H_2O(g). Ind Eng Chem Process Des Dev 18:249–254
9. De Haan DO, Finlayson-Pitts BJ (1997) Knudsen cell studies of the reaction of gaseous nitric acid with synthetic sea salt at 298 K. J Phys Chem A 101:9993–9999. doi:10.1021/jp972450s
10. Ali HM, Iedema M, Yu X-Y, Cowin JP (2014) Ionic strength dependence of the oxidation of SO_2 by H_2O_2 in sodium chloride particles. Atmos Environ 89:731–738. doi:10.1016/j.atmosenv.2014.02.045
11. Seinfeld JH, Pandis SN (1998) Atmospheric chemistry and physics: from air pollution to climate change, 1st edn. Wiley, New York
12. Herzberg G (1965) Spectra of diatomic molecules. D. Van Nostrand, Princeton, NJ
13. Ross SD (1999) Inorganic infrared and Raman spectra. McGraw-Hill, London
14. Sander R (1999) Compilation of Henry' s law constants for inorganic and organic species of potential importance in environmental chemistry. Environ Chem 29:85–107
15. Pio CA, Harrison RM (1987) The equilibrium of ammonium chloride aerosol with gaseous hydrochloric acid and ammonia under tropospheric conditions. Atmos Environ 21:1243–1246. doi:10.1016/0004-6981(87)90253-8
16. Zangmeister CD, Pemberton JE (2000) Raman spectroscopy and atomic force microscopy of the reaction of sulfuric acid with sodium chloride. J Am Chem Soc 122:12289–12296
17. Nakamoto K (1986) Infrared and Raman spectra of inorganic and coordination compounds, 4th edn. Wiley, New York
18. Barraclough PB, Hall PG (1974) The adsorption of water vapour by lithium fluoride, sodium fluoride and sodium chloride. Surf Sci 46:393–417. doi:10.1016/0039-6028(74)90316-1
19. Wassermann B, Mirbt S, Reif J et al (1993) Clustered water adsorption on the NaCl(100) surface. J Chem Phys 98:10049. doi:10.1063/1.464438
20. Dai DJ, Peters SJ, Ewing GE (1995) Water adsorption and dissociation on NaCl surfaces. J Phys Chem 99:10299–10304. doi:10.1021/j100025a035
21. Benson SW, Richardson RL (1955) The catalytic effect of water upon the addition of hydrogen chloride gas to solid sodium sulfate 1. J Am Chem Soc 77:4206–4208. doi:10.1021/ja01621a006
22. Beichert P, Finlayson-pitts BJ (1996) Knudsen cell studies of the uptake of gaseous HNO_3 and other oxides of nitrogen on solid nacl: the role of surface-adsorbed water. J Phys Chem 100:15218–15228
23. Ten Brink HM (1998) Reactive uptake of HNO_3 and H_2SO_4 in sea-salt (NaCl) particles. J Aerosol Sci 29:57–64. doi:10.1016/S0021-8502(97)00460-6